Mode Switching Is the Major Mechanism of Ligand Regulation of InsP$_3$ Receptor Calcium Release Channels

Lucian Ionescu,[1] Carl White,[1] King-Ho Cheung,[1] Jianwei Shuai,[3] Ian Parker,[3] John E. Pearson,[4] J. Kevin Foskett,[1,2] and Don-On Daniel Mak[1]

[1]Department of Physiology and [2]Department of Cell and Developmental Biology, University of Pennsylvania School of Medicine, Philadelphia, PA 19104
[3]Department of Neurobiology and Behavior, University of California, Irvine, CA 92697
[4]Theoretical Biology and Biophysics, Los Alamos National Laboratory, Los Alamos, NM 87545

The inositol 1,4,5-trisphosphate (InsP$_3$) receptor (InsP$_3$R) plays a critical role in generation of complex Ca^{2+} signals in many cell types. In patch clamp recordings of isolated nuclei from insect Sf9 cells, InsP$_3$R channels were consistently detected with regulation by cytoplasmic InsP$_3$ and free Ca^{2+} concentrations ([Ca^{2+}]$_i$) very similar to that observed for vertebrate InsP$_3$R. Long channel activity durations of the Sf9-InsP$_3$R have now enabled identification of a novel aspect of InsP$_3$R gating: modal gating. Using a novel algorithm to analyze channel modal gating kinetics, InsP$_3$R gating can be separated into three distinct modes: a low activity mode, a fast kinetic mode, and a burst mode with channel open probability (P_o) within each mode of 0.007 ± 0.002, 0.24 ± 0.03, and 0.85 ± 0.02, respectively. Channels reside in each mode for long periods (tens of opening and closing events), and transitions between modes can be discerned with high resolution (within two channel opening and closing events). Remarkably, regulation of channel gating by [Ca^{2+}]$_i$ and [InsP$_3$] does not substantially alter channel P_o within a mode. Instead, [Ca^{2+}]$_i$ and [InsP$_3$] affect overall channel P_o primarily by changing the relative probability of the channel being in each mode, especially the high and low P_o modes. This novel observation therefore reveals modal switching as the major mechanism of physiological regulation of InsP$_3$R channel activity, with implications for the kinetics of Ca^{2+} release events in cells.

INTRODUCTION

Inositol 1,4,5-trisphosphate (InsP$_3$) is a second messenger generated together with diacylglycerol by phospholipase C activated by G protein–coupled and tyrosine kinase receptors in response to extracellular stimuli (Berridge and Irvine, 1989; Berridge, 1993). The free InsP$_3$ binds to its receptor (InsP$_3$R), a ubiquitous, ER-localized Ca^{2+} channel, activating it to release Ca^{2+} from the ER lumen to increase cytoplasmic free Ca^{2+} concentration ([Ca^{2+}]$_i$). InsP$_3$-mediated [Ca^{2+}]$_i$ changes play critical roles in multiple signaling pathways and are involved in generation and regulation of multiple biological processes, including synaptic transmission, gene expression, and apoptosis. Analyses of InsP$_3$-mediated [Ca^{2+}]$_i$ signals in nonexcitable cells have revealed complex spatial and temporal features, providing highly regulated global as well as localized control of Ca^{2+}-dependent processes (Woods et al., 1986; Petersen et al., 1991; Tregear et al., 1991; Thorn et al., 1993; Bootman et al., 2002).

Characterization of InsP$_3$R channel activity and its regulation is essential for molecular insights into these intricate intracellular Ca^{2+} signaling pathways. Application of the patch clamp technique to isolated nuclei (Mak and Foskett, 1994) has provided the most direct approach to study the detailed permeation and gating properties of single InsP$_3$R ion channels in their native ER membrane environment. The endogenous InsP$_3$R of cultured insect *Spodoptera frugiperda* (Sf9) cells shares many basic properties with *Xenopus* and rat InsP$_3$R channels studied previously, including a biphasic dependence of its activity on [Ca^{2+}]$_i$ that is critical for generation of spatially and temporally complex [Ca^{2+}]$_i$ signals in cells (Ionescu et al., 2006; Foskett et al., 2007). The InsP$_3$R channel activities observed in Sf9 nuclear patches last longer than the channels in the other systems before they inevitably inactivate (Boehning et al., 2001; Mak et al., 2005; Ionescu et al., 2006). The longer activity durations of Sf9 InsP$_3$R channels provide more event transitions for gating analyses, enabling observations of novel gating behaviors over longer time scales.

Examination of extensive current records of single Sf9 InsP$_3$R channels in the presence of well-controlled and constant levels of [InsP$_3$] and [Ca^{2+}]$_i$ revealed that the channels did not display steady-state gating behavior, but instead exhibited spontaneous changes in gating kinetics through distinct patterns of behavior, or modes. We developed a new algorithm to analyze modal gating kinetics of the channel and identified three distinct

Correspondence to J. Kevin Foskett: foskett@mail.med.upenn.edu

Abbreviations used in this paper: InsP$_3$, inositol 1,4,5-trisphosphate; InsP$_3$R, InsP$_3$ receptor.

gating modes of the InsP$_3$R: a mode in which the channel is mostly bursting, another with fast channel gating kinetics, and one with long quiescent periods, with channel open probability P_o of 0.85, 0.24, and 0.007, respectively. Unexpectedly, the channel P_o within each mode remain relatively consistent over a wide range of [Ca^{2+}]$_i$ and [InsP$_3$]. Remarkably, our analysis therefore indicates that the observed biphasic [Ca^{2+}]$_i$ dependence and [InsP$_3$] regulation of InsP$_3$R channel activity are generated primarily by ligand regulation of the relative prevalence of the three gating modes.

MATERIALS AND METHODS

Sf9 Cell Culture and Nuclear Isolation
Spodoptera frugiperda (Sf9) cells (Invitrogen) were grown and maintained in SF-900II serum-free media (GIBCO BRL) in suspension culture according to the manufacturer's protocols. Each batch of cells was subcultured three to four times before being used for electrophysiology and then propagated and used for nuclear isolation for up to 7–8 wk in culture before a new lot was thawed and expanded. Nuclei were prepared for patch clamping as previously described (Ionescu et al., 2006). The nuclear preparation was added to a standard bath solution in an experimental chamber on the stage of an inverted microscope as previously described (Mak et al., 1998; Boehning et al., 2001). Isolated nuclei (5–10 μM in diameter) were distinguished from intact cells based on their unique morphology and selected for electrophysiology (Mak et al., 2005; Ionescu et al., 2006).

Data Acquisition
Nuclear patch clamping was performed as previously described (Mak et al., 1998). To maximize the duration of the observed channel activity, current recording was started as soon as seal resistance exceeded 150 MΩ. The standard pipette solution contained (in mM) 140 KCl, 10 HEPES (pH 7.3 by KOH), 0.5 Na$_2$ATP, 0.5 Ca^{2+} chelator, and various [Ca^{2+}] and [InsP$_3$], as indicated. The bath solution contained (in mM) 140 KCl, 10 HEPES (pH 7.3 by KOH), 0.5 BAPTA (1,2-bis(*O*-aminophenoxy) ethane-*N,N,N',N'*-tetraacetic acid; Molecular Probes), and 0.225 CaCl$_2$ (free [Ca^{2+}] = 300 nM). All solutions were carefully buffered to desired free [Ca^{2+}] using Ca^{2+} chelators with appropriate affinities (Mak et al., 1998), confirmed by fluorometry. All current traces used for analysis were recorded under 20 mV in room temperature. Data were acquired using an Axopatch 200B amplifier (Axon Instruments), filtered at 1 kHz, and digitized at 5 kHz with an ITC-16 interface (Instrutech) and Pulse software (HEKA Electronik).

Data Analysis
Segments of current records exhibiting current levels for a single InsP$_3$R channel under various ligand conditions (Table I) were idealized using QuB software (University of Buffalo) with SKM algorithm (Qin et al., 2000a,b). Channel gating kinetics and modal gating behaviors were characterized using our custom algorithm (Appendix) written using Igor Pro software (WaveMetrics). Statistical analyses were performed and figures were generated using Igor Pro software.

RESULTS

Application of the nuclear patch clamp technique to nuclei isolated from cultured insect Sf9 cells provided long, uninterrupted single-channel current records of the endogenous InsP$_3$R in its native ER membrane environment over a wide range of concentrations of cytoplasmic ligands (InsP$_3$ and Ca^{2+}) (Ionescu et al., 2006). With rigorous control of constant ligand and ionic conditions in the pipette and bath solutions during our experiments (Ionescu et al., 2006), we found that in all ligand conditions used, the InsP$_3$R exhibited apparent modal gating behaviors: it gated with steady kinetics for extensive periods (significantly longer than the mean open and closed channel durations) before gating abruptly changed into a discernibly different pattern. In experiments yielding single InsP$_3$R channel current records, channels were regularly observed to exhibit many such transitions through several modes of gating kinetics (Fig. 1).

Characterization of Modal Gating
To characterize this modal gating of the Sf9 InsP$_3$R channel and its regulation by [Ca^{2+}]$_i$ and [InsP$_3$], we examined thousands of seconds of single-channel current records that were obtained in many experiments in the presence of saturating (10 μM) and subsaturating (33 nM) [InsP$_3$], and subactivating (0.1 μM), optimal (1 μM), and inhibitory (89 μM) [Ca^{2+}]$_i$ (Table I). One characteristic of InsP$_3$R channel gating is the wide range of closed channel durations observed. The channels sometimes remained closed for extensive periods (seconds to tens of seconds) that were orders of magnitudes longer than other closing durations (∼10 ms). In addition, the transitions of InsP$_3$R channel gating from one mode to another occurred abruptly (Fig. 1). To avoid inherent limitations of conventional modal gating analysis algorithms, we developed a novel algorithm that is able to (a) determine when modal transitions occurred with high temporal resolution, and (b) identify the gating modes of InsP$_3$R channels in current records of arbitrary durations without the requirement to average channel kinetic parameters like channel P_o or open or closed channel durations (Appendix).

Our modal gating analysis algorithm uses insights into InsP$_3$R channel gating derived from an allosteric model previously developed to quantitatively account for single InsP$_3$R channel gating behaviors under a wide range of [InsP$_3$] and [Ca^{2+}]$_i$: that open InsP$_3$R channels close either via brief ligand-independent closings or via closings with durations regulated by [InsP$_3$] and [Ca^{2+}]$_i$ (Mak et al., 2003). Because the ligand regulation of InsP$_3$R channel gating is of primary interest, burst analysis was used (Magleby and Pallotta, 1983a) in the channel gating analysis to remove the majority of the brief ligand-independent channel closings so that kinetics of the ligand-dependent channel gating can be more easily discerned (Appendix and Table II therein). After burst analysis, the remaining channel openings and closings should be predominantly due to ligand-regulated channel gating. For clarity, those channel openings are referred to as
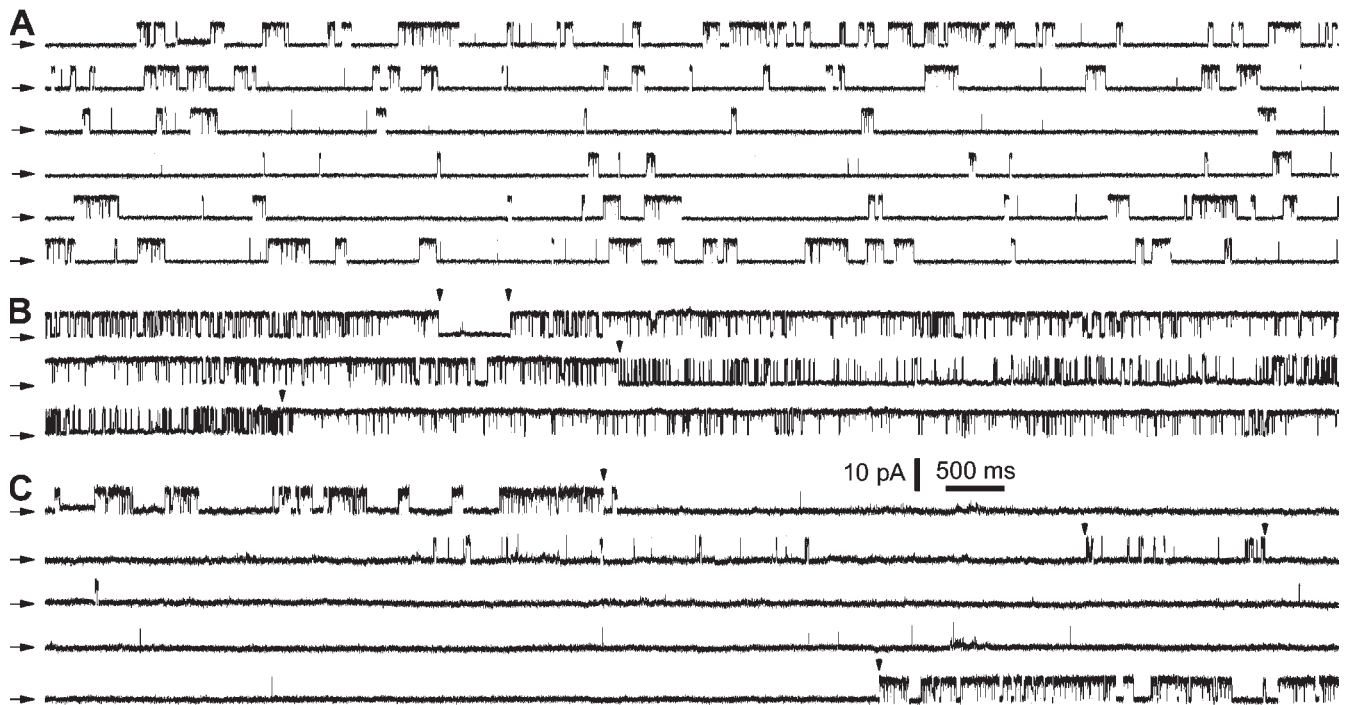
Figure 1. Single InsP₃R channel current traces showing long-term modal gating behavior. Current records were obtained with [InsP₃] = 10 μM (saturating), and [Ca²⁺]ᵢ = (A) 100 nM, (B) 1 μM, and (C) 89 μM. A continuous current record is shown for each condition. The arrows on the left indicate the closed-channel background current levels for this and all subsequent current traces. In B and C, arrowheads indicate some transitions when the InsP₃R channel gating behavior changed discernibly.

bursts with durations t_b, separated by burst-terminating gaps with durations t_g.

Based on the values of t_b and t_g of adjacent burst-gap pairs, our algorithm consistently identified three distinct gating patterns (modes) in all the InsP₃R channel current traces obtained in all [Ca²⁺]ᵢ and [InsP₃] examined (Appendix). In the gating mode with high P_o (H mode), the channel exhibits mainly bursting behavior with only brief gaps interrupting the long bursts of channel activity (Fig. 2, A and D). In the gating mode with intermediate P_o (I mode), the InsP₃R channel gates frequently with mostly short openings and closings (Fig. 2, B and E). In the low-P_o (L mode), the channel has long closed periods interrupted with brief, infrequent openings, so channel P_o is very low (Fig. 2, C and F).

[Ca²⁺]ᵢ Regulation of Modal Gating

Single Sf9 InsP₃R channel current records obtained in saturating 10 μM InsP₃ under three different [Ca²⁺]ᵢ (0.1, 1, and 89 μM) were examined for modal gating behaviors. As observed during the basic characterization of the channel gating properties (Ionescu et al., 2006), the three [Ca²⁺]ᵢ covered the full range of biphasic InsP₃R channel responses under saturating [InsP₃]: in [Ca²⁺]ᵢ = 0.1 μM, the InsP₃R channel is suboptimally activated by Ca²⁺ so channel P_o is low (~0.1); in [Ca²⁺]ᵢ = 1 μM, the channel is optimally activated by Ca²⁺ with high channel P_o (~0.6–0.8); and in [Ca²⁺]ᵢ = 89 μM, the channel is inhibited by high [Ca²⁺]ᵢ so that channel P_o is again low (~0.1) (Fig. 3 A). In agreement with the previous characterization, the [Ca²⁺]ᵢ dependence of channel P_o is mainly reflected in changes in mean closed

TABLE I
Statistics of Data Analyzed

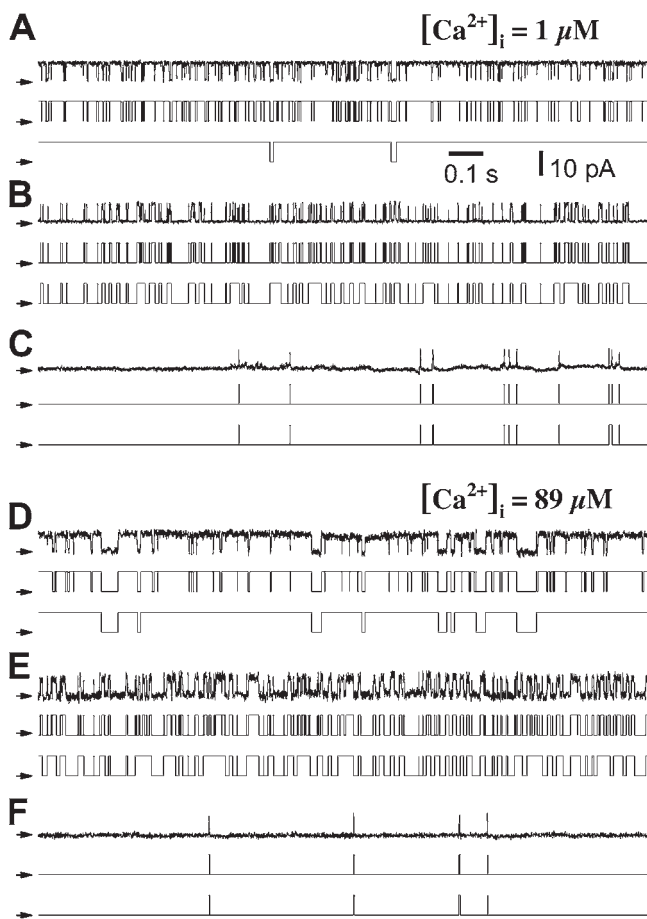| [Ca²⁺]ᵢ	[InsP₃]	Number of membrane patches	Total record duration	Mean duration per patch[a]	Total opening events	Mean opening events per patch[a]
μM	*μM*		*s*	*s*		
0.1	10	16	2882.3	180 ± 49	14,775	923 ± 292
1	10	26	3394.2	131 ± 28	157,925	6,074 ± 1,875
89	10	18	1483.5	82 ± 41	15,512	862 ± 222
1	0.033	15	656.0	42 ± 7	11,850	790 ± 260

[a]Mean ± SEM are tabulated.

Figure 2. Distinct patterns of InsP$_3$R channel gating in each of the three modes as revealed by burst filtering. The current records were obtained in saturating 10 μM InsP$_3$ and [Ca^{2+}]$_i$ as tabulated. Each section consists of a set of three traces of the same single channel current record: (top) unprocessed current trace, (middle) idealized current trace generated from current record using Qub software, and (bottom) idealized current trace after burst analysis. (A) InsP$_3$R gating in high-P_o, H, mode in which the channel opens mainly in bursts whose gating behavior is substantially affected by burst analysis. (B) InsP$_3$R gating in intermediate-P_o, I, mode with rapid opening and closing kinetics that is largely unaffected by burst analysis. (C) Channel gating in low-P_o, L, mode with brief openings separated by very long closed durations.

channel duration $\langle t_c \rangle$ over more than an order of magnitude as [Ca^{2+}]$_i$ was changed, while mean open channel duration $\langle t_o \rangle$ remained relatively constant in all [Ca^{2+}]$_i$ (Fig. 3 E).

Examination of the gating properties of the InsP$_3$R channel during the periods in which the channel remained in a particular gating mode revealed that the channel P_o within each gating mode (P_o^M, with M standing for H, I, or L) has a distinct value 0.85 ± 0.02, 0.24 ± 0.03, and 0.007 ± 0.002 for the H, I, and L modes, respectively, that remains surprisingly consistent over all [Ca^{2+}]$_i$ examined (Fig. 3 B). Because the modal gating analysis algorithm assigns modes only by the values of

t_g and t_c after burst analysis, without directly taking into account the channel P_o (Appendix), the consistency of the channel P_o^M over the various ligand concentrations strongly suggests that the gating modes detected are true representations of the gating kinetics of the channel and not an artifact of the analysis protocol.

Because the InsP$_3$R channel P_o within a mode (P_o^M) exhibited relatively small [Ca^{2+}]$_i$ dependencies, [Ca^{2+}]$_i$ must regulate the overall channel P_o predominantly by regulating the fraction of time the channel spends in the different gating modes (relative prevalence π^M) (Fig. 3 C). Examination of modal kinetics revealed that π^I is comparatively [Ca^{2+}]$_i$ independent (Fig. 3 C); the frequency of the channel entering the I mode (relative modal frequency f^I) (Fig. 3 D) as well as the mean modal dwell time $\langle \tau^I \rangle$ of the channel in the I mode (Fig. 3 J) exhibited very little [Ca^{2+}]$_i$ dependence. In contrast, both π^H and π^L showed profound ligand dependencies. In the presence of saturating 10 μM InsP$_3$ and optimal 1 μM [Ca^{2+}]$_i$, the InsP$_3$R channel is found most of the time in the H mode with high P_o^H, and in the L mode for relatively little time (Fig. 3 C), resulting in the observed high overall channel activity (Fig. 3 A). The high π^H observed is due to the channel entering the H mode more frequently (higher f^H, Fig. 3 D) and staying in that mode longer (higher $\langle \tau^H \rangle$, Fig. 3 J). In nonoptimal [Ca^{2+}]$_i$ (0.1 and 89 μM), the channel has low overall activity (Fig. 3 A) mainly because it enters the L mode more frequently (higher f^L, Fig. 3 D). Unlike $\langle \tau^H \rangle$, which exhibits a strong [Ca^{2+}]$_i$ dependence, $\langle \tau^L \rangle$ remains within a relatively narrow range in all [Ca^{2+}]$_i$ (Fig. 3 J).

Although InsP$_3$R channel P_o^M stayed within a narrow range over all [Ca^{2+}]$_i$ examined, the gating kinetics within a mode are not [Ca^{2+}]$_i$ independent. The channel open, closed, burst, and gap duration distributions in the three modes ($\langle t_o^M \rangle$, $\langle t_c^M \rangle$, $\langle t_b^M \rangle$, and $\langle t_g^M \rangle$, respectively) all exhibited statistically significant variations over the [Ca^{2+}]$_i$ range examined (Fig. 3, F–I).

[InsP$_3$] Regulation of Modal Gating

InsP$_3$R channel gating is regulated by [InsP$_3$] as well as by [Ca^{2+}]$_i$. It has been established that [InsP$_3$] regulates InsP$_3$R channel gating by tuning the sensitivity of the channel to inhibition by high [Ca^{2+}]$_i$ (Mak et al., 1998, 2001; Ionescu et al., 2006). Thus, in the presence of subsaturating [InsP$_3$] (33 nM), the Sf9 InsP$_3$R channel is inhibited at a relatively low [Ca^{2+}]$_i$ so that P_o at [InsP$_3$] = 33 nM and [Ca^{2+}]$_i$ = 1 μM is lower than that at saturating [InsP$_3$] = 10 μM and [Ca^{2+}]$_i$ = 1 μM (Fig. 3 A). This reduction in channel P_o is mainly due to increases in $\langle t_c \rangle$ whereas $\langle t_o \rangle$ shows little dependence on [InsP$_3$] (Fig. 3 E). Modal analysis of InsP$_3$R channel current records obtained in [InsP$_3$] = 33 nM and [Ca^{2+}]$_i$ = 1 μM revealed that the channels in subsaturating (33 nM) [InsP$_3$] exhibit the same three gating modes (H, I, and L modes) with very similar P_o^M in each of the modes as
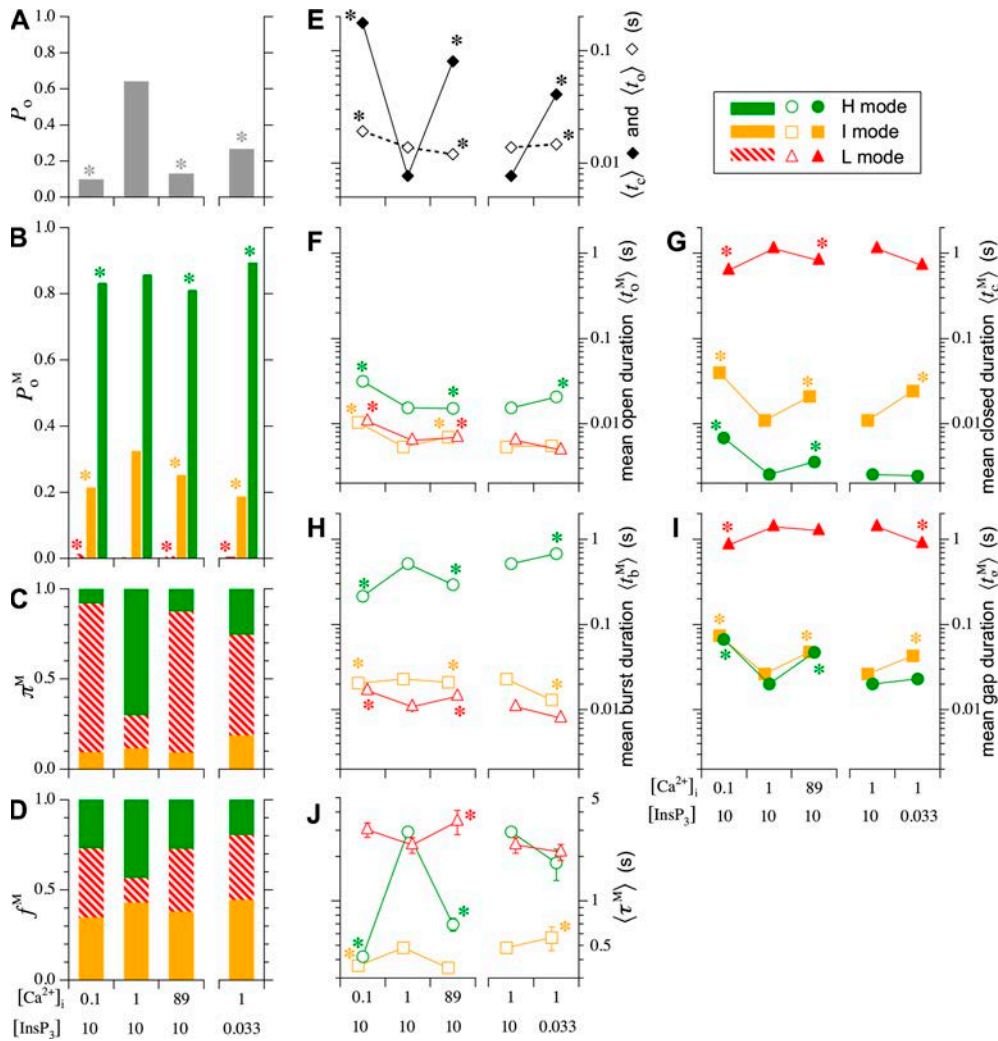
Figure 3. InsP$_3$R channel gating parameters observed in various [Ca^{2+}]$_i$ and [InsP$_3$] as tabulated (in μM). All parameters plotted were evaluated using event-based statistics (See Appendix). (A) Channel open probability P_o. (B) Channel open probability in each of the three channel gating modes P_o^M (M stands for H, I, or L, depending on the mode involved). Parameters for the H, I, and L modes are plotted in bar graphs (B–D) in green, yellow, and red, respectively, as indicated by the Key on the upper right corner. (C) Relative prevalence π^M (amount of time the channel spent in a mode/total duration of all analyzed channel current records) for the three gating modes. (D) Relative frequency f^M (number of times the channel entered a mode/total numbers of modal transitions in all current records) of the gating modes. (E) Mean channel opening $\langle t_o \rangle$ (open diamonds) and closing $\langle t_c \rangle$ (filled diamonds) duration overall. (F–I) Mean durations of channel opening $\langle t_o^M \rangle$, closing $\langle t_c^M \rangle$, bursts $\langle t_b^M \rangle$, and burst-terminating gaps $\langle t_g^M \rangle$, respectively, for the gating modes. Error bars in bar graphs (A and B) are too small to be plotted noticeably, and those in graphs (E–I) are smaller than the symbols (see Appendix). (J) Mean duration $\langle \tau^M \rangle$ of the gating modes. Color and symbols used in graphs (F–J) for the gating modes are tabulated in the key on the upper right corner. Note that in graphs (E–J), the gating kinetic parameters for optimal channel activity ([Ca^{2+}]$_i$ = 1 μM and [InsP$_3$] = 10 μM) are plotted in the left panel for varying [Ca^{2+}]$_i$ as well as in the right panel for varying [InsP$_3$] for easier comparison. Parameters marked with asterisks are those observed in suboptimal ligand concentrations that are statistically significantly different from those observed in optimal [Ca^{2+}]$_i$ (1 μM) and saturated [InsP$_3$] (10 μM).

compared with channels in saturating (10 μM) [InsP$_3$] (Fig. 3 B). Regulation of the overall channel P_o by [InsP$_3$] is therefore mediated by the effects of [InsP$_3$] on π^M, which agrees with the observation that in subsaturating [InsP$_3$], the channel is inhibited by lower [Ca^{2+}]$_i$ (Fig. 3 C). In 33 nM [InsP$_3$] and 1 μM [Ca^{2+}]$_i$, π^I is not very different from that for the channel in saturating (10 μM) [InsP$_3$]. The ratio of π^H: π^L in [Ca^{2+}]$_i$ = 1 μM and [InsP$_3$] = 33 nM is smaller than that for a channel in the same [Ca^{2+}]$_i$ but saturating 10 μM [InsP$_3$], as inhibition by Ca^{2+} stabilizes the L mode relative to the H mode. Since the gating kinetic properties ($\langle t_o^M \rangle$, $\langle t_c^M \rangle$, $\langle t_b^M \rangle$, and $\langle t_g^M \rangle$) of the channel in each mode are significantly regulated by [Ca^{2+}]$_i$, and InsP$_3$ regulates InsP$_3$R channel activity by altering the sensitivity of the channel to Ca^{2+} regulation, these gating kinetic prop-

erties of the channel in each mode display dependence on [InsP$_3$], as expected (Fig. 3, F–I).

DISCUSSION

We have here obtained long single-channel current records with robust InsP$_3$R channel activities over a wide range of [Ca^{2+}]$_i$ and [InsP$_3$] by patch clamp electrophysiology of isolated nuclei from Sf9 cells. These records have provided new insights into the gating behavior of the InsP$_3$R channel. InsP$_3$R gating is modal, with three distinct patterns of activity identified. Importantly, ligand regulation of channel activity impinges directly upon this modal gating behavior, with Ca^{2+} and InsP$_3$ regulating the propensity of the channel to be in each of the three stereotypic, relatively ligand-independent modes.

The InsP$_3$R Channel Gates in Three Modes

Based on an allosteric model that quantitatively accounted for single InsP$_3$R channel gating behaviors under a wide range of [InsP$_3$] and [Ca^{2+}]$_i$ (Mak et al., 2003), a novel algorithm was developed to determine the gating mode of the InsP$_3$R with high temporal resolution and little ambiguity (Appendix and Figs. 4–6 therein). Our modal gating analysis determined that the InsP$_3$R channel gates with three different gating modes, each exhibiting distinct gating kinetics (Figs. 3 and 7 in Appendix). Although our algorithm is different from conventional modal analyses, which assign gating modes based on the average of some channel kinetic parameter (Blatz and Magleby, 1986; McManus and Magleby, 1988; Delcour and Tsien, 1993; Delcour et al., 1993; Catacuzzeno et al., 1999; Saftenku et al., 2001; Popescu and Auerbach, 2003; Popescu et al., 2004), its validity was confirmed by the clear separation of the values of channel P_o within the three gating modes in all [Ca^{2+}]$_i$ examined (Fig. 3 C) despite the fact that channel P_o was not directly taken into consideration in the modal analysis algorithm.

Examination of the modal transitions identified by our modal analysis algorithm revealed that spontaneous transitions from any one of the modes into the other two occurred regularly despite the fact that the channels were exposed to constant levels of [InsP$_3$] and [Ca^{2+}]$_i$ during each experiment. Modal gating of ion channels cannot be accounted for by simple kinetic schemes that are linearly connected (Delcour and Tsien, 1993; Zahradnikova and Zahradnik, 1996). Rather, the observed interconnectivity between modes can only be accounted for by more complex, tiered kinetic schemes in which each mode has its own independent set (tier) of connected open and closed kinetic states, and the three tiers for the three modes are completely interconnected, as previously depicted (Delcour et al., 1993; Popescu and Auerbach, 2003; Popescu and Auerbach, 2004; Popescu et al., 2004); or by kinetic schemes with a loop, as previously depicted (Zahradnikova and Zahradnik, 1996, 1999; Saftenku et al., 2001; Rosales et al., 2004). Thus, among the various kinetic models that have been proposed to account for InsP$_3$R-mediated Ca^{2+} signaling, the ones involving just a single explicit open channel kinetic state (for example see De Young and Keizer, 1992; Atri et al., 1993; Othmer and Tang, 1993; Bezprozvanny, 1994; Bezprozvanny and Ehrlich, 1994; Swillens et al., 1994; Dupont and Swillens, 1996; Marchant and Taylor, 1997; Hirose et al., 1998; Swillens et al., 1998; Adkins and Taylor, 1999; Swillens et al., 1999; Sneyd and Dufour, 2002; Swatton and Taylor, 2002), cannot describe the modal gating behaviors observed in this study. Only kinetic models in which the InsP$_3$R channel has multiple independent open-to-closed transitions (Bruno et al., 2005) (for example see Kaftan et al., 1997; Moraru et al., 1999; Dawson et al., 2003;

Mak et al., 2003; Fraiman and Dawson, 2004) have the potential to account for the observed modal gating behaviors. However, since all these models were developed to account for steady-state channel gating behavior under constant [InsP$_3$] and [Ca^{2+}]$_i$, they all need to be substantially expanded to describe the modal gating behaviors of the InsP$_3$R channel in which spontaneous transitions from one gating mode to another occurred regularly even in the presence of constant [InsP$_3$] and [Ca^{2+}]$_i$. As a starting point, we present in the Appendix (and Fig. 8 therein) the simplest model that quantitatively accounts for the InsP$_3$R channel modal gating behaviors observed.

Ligand Regulation of InsP$_3$R Channel Activity Is Mainly Mediated through Mode Switching

A surprising result of our modal analysis is that ligand regulation of InsP$_3$R channel activity (P_o), a critical aspect of regulation of InsP$_3$-mediated intracellular Ca^{2+} signaling, is mediated mainly by ligand regulation of the relative prevalence of the H mode vs. the L mode (Fig. 3 C). Within the range of [Ca^{2+}]$_i$ and [InsP$_3$] examined, all the kinetics of the I mode (relative prevalence π^I, relative frequency f^I, and mean dwell time $\langle \tau^I \rangle$) exhibit little [Ca^{2+}]$_i$ or [InsP$_3$] dependencies (Fig. 3, C, D, and J). Mode switching is not the only mechanism for ligand regulation of InsP$_3$R channel kinetics, because detailed gating kinetics of the channel in individual modes ($\langle t_o^M \rangle$ and $\langle t_c^M \rangle$) are also significantly regulated by [InsP$_3$] and [Ca^{2+}]$_i$. We suggest that mode switching is nevertheless the most relevant mechanism of ligand regulation of InsP$_3$R-mediated Ca^{2+} release. InsP$_3$R channels are spatially localized in the ER in clusters (Mak and Foskett, 1994; Ionescu et al., 2006) with more than one active channel involved in the generation of various Ca^{2+} signaling events ranging from blips and puffs to propagating saltatory waves (Yao et al., 1995; Foskett et al., 2007). Because the opening and closing kinetics of individual channels are averaged out over the multiple active channels involved, it is the P_o of the active InsP$_3$R channels that directly govern the amount of Ca^{2+} released and therefore the characteristics of the Ca^{2+} signal generated. Thus, ligand-dependent mode switching, which directly impinges on the channel P_o, is the major mechanism for ligand regulation of InsP$_3$-mediated Ca^{2+} signals. Deeper understanding of the kinetic mechanisms responsible for modal gating behaviors of the channel will therefore provide further insights into ligand regulation of InsP$_3$R-mediated Ca^{2+} signaling.

Physiological Significance of InsP$_3$R Modal Gating

Modal gating kinetics have been observed in many different ion channels, including Cl$^-$ channels (Blatz and Magleby, 1986; Catacuzzeno et al., 1999), "maxi" BK (Magleby and Pallotta, 1983a,b; McManus and Magleby,

1988; Rothberg et al., 1996), G protein–activated (Yakubovich et al., 2000) channels, NMDA (Popescu and Auerbach, 2003; Popescu et al., 2004) and nicotinic (Auerbach and Lingle, 1986; Naranjo and Brehm, 1993) receptors, N- (Delcour and Tsien, 1993; Delcour et al., 1993), P/Q- (Luvisetto et al., 2004), and L-type (Imredy and Yue, 1994) Ca^{2+} channels, to name a few. Although different channel gating modes have been associated with distinct long-term channel kinetic features, including inactivation (Imredy and Yue, 1994), desensitization (Naranjo and Brehm, 1993), ligand inhibition (Delcour and Tsien, 1993), and quantitative features of subunit modulation (Luvisetto et al., 2004), the physiological significance of modal gating is in most cases not clear. Modal gating has also been observed in ryanodine receptors (RyRs), the other major intracellular Ca^{2+} release channel with sequence homologies with $InsP_3R$, where it has been proposed to contribute to "adaptation" behavior of RyR in response to $[Ca^{2+}]_i$ jumps (Zahradnikova and Zahradnik, 1996; Zahradnikova et al., 1999; Fill et al., 2000; Rosales et al., 2004). However, the physiological significance of "adaptation" is also not clear, and the $InsP_3R$ does not display similar "adaptation" behaviors in response to rapid changes in $InsP_3$ or Ca^{2+} concentrations (Mak et al., 2007). The results here, by demonstrating that important ligand regulation of $InsP_3R$ channel activity impinges primarily on modal gating, provide a clear demonstration of the physiological relevance of channel modal gating.

The modal gating analysis presented here was performed on single-channel current traces from insect Sf9 $InsP_3R$ mainly because these channels remain active for long extensive periods during nuclear patch clamp experiments (mean channel activity duration ∼120 s; Ionescu et al., 2006). In retrospect, it appears that modal gating behavior was previously observed in nuclear patch-clamp records of diverse endogenous or recombinant channels from different $InsP_3R$ isoforms (type 1 and 3) and splice variants (SII+/−) of different species (*Xenopus laevis* frogs and rat). Bursts of high channel activities (H mode) separated by long quiescent periods (L mode) were observed in endogenous *Xenopus* type 1 $InsP_3R$ channels (Mak and Foskett, 1997; Mak et al., 1998). Single-channel current records of recombinant rat type 3 $InsP_3R$ expressed in *Xenopus* oocytes presented by Mak et al. (2000, 2001) are reminiscent of the Sf9 $InsP_3R$ channel current records exhibiting modal gating behaviors presented here (Fig. 2). Current records of recombinant rat type 1 $InsP_3R$ channels expressed in mammalian COS-7 cells presented by Boehning et al. (2001) clearly exhibited the three gating modes. Furthermore, biphasic regulation of the relative prevalence of the H mode by Ca^{2+} paralleling the biphasic Ca^{2+} regulation of $InsP_3R$ channel activity that is reported here was also clearly observable in the current records obtained in various $[Ca^{2+}]_i$ for different $InsP_3R$ isoform

channels from different species (Mak et al., 1998, 2001; Boehning et al., 2001). Thus, although a comprehensive study of modal gating behavior (like the one performed here for the Sf9 $InsP_3R$ channels) was not feasible for the other $InsP_3R$ channels because of their short channel activity durations due to channel rundown or inactivation (Mak and Foskett, 1997; Mak et al., 2000; Boehning et al., 2001), modal gating appears to have been widely observed in many different types of $InsP_3R$ and probably plays a major role in ligand regulation of many if not all $InsP_3R$ channels.

The important role modal gating plays in ligand regulation of $InsP_3R$ activity indicates that besides the time scales of channel openings and closings (t_o and $t_c \sim$ ms, Fig. 3 E), other, longer time scales in $InsP_3R$ channel gating kinetics are likely to be relevant for the kinetics of $InsP_3$-mediated intracellular Ca^{2+} signaling in vivo. One such time scale is associated with the channel burst (t_b) and burst-terminating (interburst) gap (t_g) durations. Whereas most of the short channel closings are the result of ligand-independent channel gating (Mak et al., 2003; Foskett and Mak, 2004), the time scales of the bursts and gaps probably reflect the kinetics of ligand unbinding from and binding to, respectively, the channel and the associated $InsP_3R$ conformational changes. This assumption is supported by the results of the modal gating analysis here (Appendix and Table II therein). Thus, the durations of the bursts and gaps, rather than the durations of channel opening and closing, probably provide a better measure of the kinetics of the response of the $InsP_3R$ channel to ligand concentration changes.

A recent study of the kinetic responses of single $InsP_3R$ channels to rapid ligand concentration changes observed that in the constant presence of saturating 10 μM $InsP_3$, the mean lag times to termination of $InsP_3R$ channel activity from abrupt changes in $[Ca^{2+}]_i$ from optimal (2 μM) to subactivating (<10 nM) and/or inhibitory (300 μM) levels were 160 and 290 ms, respectively. In constant 2 μM Ca^{2+}_i, the mean lag time to channel activity termination from an abrupt drop in $[InsP_3]$ from 10 μM to 0 was 700 ms (Mak et al., 2007). In those experiments, the channels were most likely in the H mode before the activity-terminating ligand concentration change, with mean burst duration $\left\langle t_b^H \right\rangle$ of 200–600 ms (Fig. 3 H). The similarity between the mean channel lag times observed in rapid perfusion experiments and the mean burst duration determined here suggests that the kinetics of channel responses to changes in ligand concentrations are likely determined by how fast the channel can exit from a burst when the ligand concentration change occurs. If that is the case, then instead of a channel opening, a channel burst probably constitutes a stereotypical single-channel $InsP_3R$ Ca^{2+}-release event.

The weak dependence of channel burst duration on $[Ca^{2+}]_i$ may possibly be a mechanism by which an active

InsP$_3$R channel can avoid being prematurely inhibited by the Ca^{2+} that it releases, because an increase of [Ca^{2+}]$_i$ from 1 μM (optimal) to 89 μM (inhibitory) only reduces the burst duration from ~500 to ~300 ms when the channel is in H mode (Fig. 3 H). Moreover, the stabilization by activating [Ca^{2+}]$_i$ of the H mode (Fig. 3 J), which has significantly longer burst durations (Fig. 3 H), may possibly play an important role in Ca^{2+}-induced Ca^{2+} release. Thus, in the presence of sufficiently high [InsP$_3$], an increase in [Ca^{2+}]$_i$ above the resting level can encourage an InsP$_3$R channel to enter the H mode from the L mode. As a result, the burst duration of the channel increases from that for an L mode (~10 ms), which may not release enough Ca^{2+} to recruit nearby channels to propagate a Ca^{2+} signal (individual blips or puffs) to that of an H mode (~200 ms), which enables the InsP$_3$R channel to continue releasing Ca^{2+} even when the local [Ca^{2+}]$_i$ is raised to a high level. Such long channel bursts can release sufficient Ca^{2+} to recruit neighboring InsP$_3$Rs or InsP$_3$R clusters for a regenerative Ca^{2+} signal (Berridge, 1997; Ionescu et al., 2006).

In summary, we have demonstrated that the InsP$_3$R gates with stereotypic behaviors in three distinct modes, and that mode switching accounts for most of the ligand regulation of InsP$_3$R Ca^{2+} release channel. Modal switching is therefore a novel major mechanism of physiological regulation of InsP$_3$R channel activity, with implications for the kinetics of Ca^{2+} release events in cells.

APPENDIX

New Algorithm Needed to Analyze Modal Gating Kinetics of InsP$_3$R Channels

Conventional modal gating analysis algorithms assign modes according to the value of a channel kinetic parameter, e.g., P_o, or channel opening or closing durations, averaged over current record segments either with a fixed duration (Delcour and Tsien, 1993; Delcour et al., 1993; Saftenku et al., 2001; Popescu and Auerbach, 2003; Popescu et al., 2004) or containing a fixed number of channel openings and closings (Blatz and Magleby, 1986; McManus and Magleby, 1988; Catacuzzeno et al., 1999). The InsP$_3$R channel exhibited closed channel durations that span several orders of magnitude (a few milliseconds to tens of seconds) in all ligand conditions examined (Fig. 1). Furthermore, the transitions between different gating patterns of the InsP$_3$R channel were abrupt (Fig. 1). Consequently, when short averaging segments were used in conventional algorithms, the value of the averaged parameter fluctuated wildly from segment to segment due to the small number of gating events present in each segment available for averaging, rendering separation of gating modes impossible. Conversely, using long averaging segments in conventional algorithms resulted in loss of temporal resolution and

failure to capture the abrupt nature of the modal transitions. Thus, we developed a novel modal gating algorithm to determine the gating mode of the InsP$_3$R channel from its current record with high accuracy and high temporal resolution.

Burst Analysis of Idealized Single-Channel InsP$_3$R Channel Current Traces

Previous analyses of the gating kinetics of various InsP$_3$R channels have revealed that the regulation of channel P_o by [Ca^{2+}]$_i$ and [InsP$_3$] is predominantly accounted for by ligand regulation of the mean channel closed duration $\langle t_c \rangle$ (Mak et al., 1998, 2001; Ionescu et al., 2006). In addition, the maximum channel P_o is ~0.8, significantly <1, even under optimal ligand conditions, when the channel gates mainly with short openings (channel open duration t_o ~10 ms) separated by very brief closings (channel closed duration t_c ~1 ms). It was previously suggested that open InsP$_3$R channels can close either via ligand-independent or -dependent conformational transitions (Mak et al., 2003), with closures under optimal ligand conditions mediated predominantly via ligand-independent transitions. By visual inspection of current records of the Sf9 InsP$_3$R channel, we surmised that such ligand-independent transitions accounted for the majority of channel closings in one of the channel gating modes. To properly identify such a gating mode, we performed a burst analysis (Magleby and Pallotta, 1983a) to remove brief channel closings that probably originated from these ligand-independent transitions. Because the ligand-dependent channel closings occur more frequently under ligand conditions that engender low channel P_o, channel closed duration distributions under such conditions are more likely to reveal a clear segregation of the two populations of channel closings originating from ligand-dependent and -independent conformation transitions. The InsP$_3$R channel t_c distribution (Fig. 4) for all current records obtained in [Ca^{2+}]$_i$ = 0.1 μM, when P_o was low, suggested that 10 ms is a reasonable value for the minimum duration of a burst-terminating gap T_{gmin} (Magleby and Pallotta, 1983a). Therefore, all channel closings with $t_c \leq T_{gmin}$ = 10 ms were considered to be caused by ligand-independent channel conformation transitions, and were removed in our burst analysis as if they never occurred. Consequently, all channel closings have durations >10 ms after the burst analysis. Those channel openings that remained after burst analysis, presumably resulting from ligand-dependent transitions, are referred to as bursts with duration t_b, separated by burst-terminating gaps with duration t_g > 10 ms. Burst analysis with T_{gmin} = 10 ms was applied to all idealized single InsP$_3$R channel current records obtained in [Ca^{2+}]$_i$ = 0.1, 1, and 89 μM.

It should be noted that even when channel exhibited low P_o in 10 μM InsP$_3$ and 0.1 μM Ca^{2+}, the duration
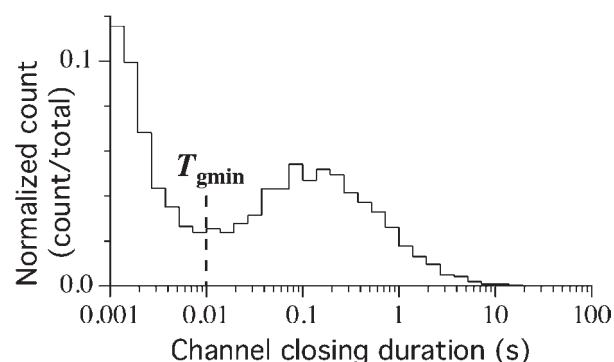
Figure 4. Logarithmic histogram of InsP$_3$R channel closing duration distribution for all experiments performed in 10 µM InsP$_3$ and $[Ca^{2+}]_i$ = 0.1 µM. T_{gmin} is the minimum burst-terminating gap duration used for burst analysis.

distribution of the short channel closing events assumed to be caused by ligand-independent conformation transitions and that of the longer channel closing events supposed to be caused by ligand-dependent transitions overlap substantially (see Fig. 4). With no information about the conformation transitions other than their durations, we applied an abrupt cut-off criterion to separate the channel closing events into two populations, one (with $t_c \le T_{gmin}$ = 10 ms) to be filtered out in our burst filtering protocol and one (with $t_c > T_{gmin}$) retained. Under the circumstances, there is no "ideal" choice of the value of T_{gmin}. Any choice of T_{gmin} will inevitably leave a population of closings with t_c just $< T_{gmin}$, which, upon visual inspection, seem long enough to be retained, and a population of closings with t_c just $> T_{gmin}$, which seem to be short enough to be filtered out. Our choice of T_{gmin} as indicated in Fig. 4 minimized the number of such "ambiguous" closings for channels in 10 µM InsP$_3$ and 0.1 µM Ca^{2+}.

The incomplete segregation of the short ligand-independent channel closings and the longer, ligand-dependent ones even in 0.1 µM Ca^{2+} and 10 µM InsP$_3$ when channel P_o is low (Fig. 4) also means that because of the stochastic nature of channel gating, a fraction of the ligand-dependent channel closings have short durations. Consequently, they are indistinguishable from the ligand-independent ones and are removed by the burst analysis. To gauge how well the abrupt cut-off criterion ($t_c <$ 10 ms) worked to remove only short channel closings that were due to ligand-independent transitions, the frequencies of short closing removal were evaluated under different ligand conditions. Assuming that separate independent mechanisms are responsible for generating ligand-independent and ligand-dependent channel closings, ligand-independent channel closings are only observable when the channel is not already closed by ligand-dependent mechanism(s). Ideally, if all ligand-independent closings can be identified, the frequency of ligand-independent closings (the number of

such channel closings observed)/(total duration of all bursts after all such closings have been removed) should remain the same under all ligand concentrations. The frequencies of short closings removed by burst analysis of current records obtained under various ligand conditions are tabulated in Table II. Although the frequencies of removed short channel closings are not completely ligand independent, they are not very different from one another, considering the experiment-to-experiment variability. This suggests that the burst analysis using an abrupt cut-off criterion, while obviously imperfect, did remove a substantial fraction of the ligand-independent short channel closings to reveal the underlying modal channel gating kinetics with considerably longer time scales (Figs. 2 and 3) without filtering out too many ligand-dependent closings.

Three Modes of InsP$_3$R Channel Gating

After burst analysis, three distinct patterns (modes) of InsP$_3$R channel gating were revealed in all $[Ca^{2+}]_i$. The channel gating kinetics in each mode were not significantly affected by the burst analysis. In the first mode, the channel has long bursts interrupted with gaps that are relatively brief (though >10 ms) so channel P_o is high (Fig. 2, A and D). In the second mode, the InsP$_3$R channel gates frequently with mostly short openings and closings, so channel P_o is moderate (Fig. 2, B and E). In the third mode, the channel has long closed periods interrupted with brief, infrequent openings, so channel P_o is very low. Burst analysis does not significantly affect the kinetics of this mode (Fig. 2, C and F). Based on their kinetic characteristics, we refer to the three InsP$_3$R channel gating patterns as the high- (H), intermediate- (I), and low- (L) activity modes, respectively.

Detection of Modal Transitions and Gating Mode Assignment

To identify with high temporal resolution changes among the gating modes of the InsP$_3$R channel (modal transitions), durations of channel bursts and burst-terminating gaps (t_b and t_g) in idealized, burst-analyzed single channel records were monitored. Either t_g or t_b crossing over some predefined abrupt thresholds T_g
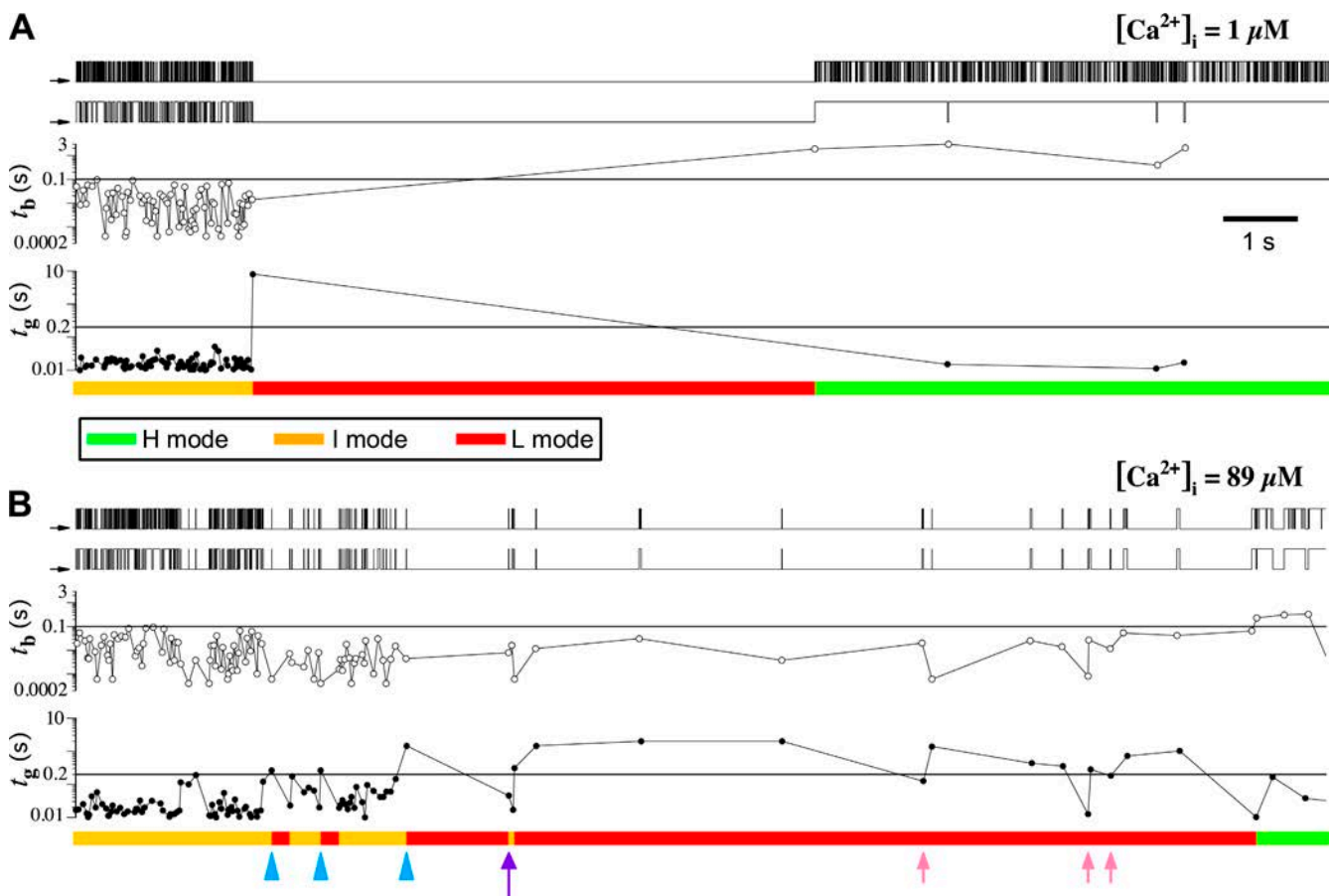
Figure 5. Identification of InsP$_3$R channel gating modes based on channel opening and closing durations. The single InsP$_3$R channel current records were obtained in saturating 10 μM InsP$_3$, and optimal (1 μM) and nonoptimal (89 μM) [Ca^{2+}]$_i$ as tabulated. Each section consists of a set of five graphs derived from the same channel record. From the top: idealized current trace, idealized current trace after burst analysis, plot of channel burst duration t_b vs. time when the channel opens, plot of channel gap duration t_g vs. time when the channel closes, and the gating mode of the channel, determined as described in the text, with green, yellow, and red representing H, I, and L modes, respectively. The current traces were selected to show modal transitions among all three gating modes in one continuous recording under various [Ca^{2+}]$_i$.

and T_b, respectively, from above or below, could signify a modal transition. Visual examination of idealized current traces (both before and after burst analysis) together with plots of t_g and t_b for all single channel current records indicated that setting $T_b = 100$ ms and $T_g = 200$ ms allowed objective detection of channel modal transitions that correlated closely with observed changes in the patterns of channel gating kinetics (Fig. 5). Because a majority of burst-terminating gaps had $t_g \le 200$ ms in all ligand conditions examined, a hysteresis requirement was implemented in the modal transition detection protocol to avoid overfragmenting the channel gating modes. Thus, a modal transition was recognized only when two or more consecutive burst-terminating gaps had $t_g \le 200$ ms following one or several consecutive gaps with $t_g > 200$ ms (long purple arrow in Fig. 5 B), but not when just one gap had t_g dropping below 200 ms (short pink arrows in Fig. 5 B). However, a modal transition was recognized when a single burst-terminating gap with $t_g > 200$ ms followed one or several consecutive

gaps with $t_g \le 200$ ms (blue arrowheads in Fig. 5 B). Similarly, a majority of channel bursts had $t_b \le 100$ ms in all ligand conditions examined. Therefore, whereas a modal transition was registered when a single channel burst had $t_b > 100$ ms following a series of bursts with $t_b \le 100$ ms, a modal transition was only registered when two consecutive channel bursts had $t_b \le 100$ ms following a series of bursts with $t_b > 100$ ms.

After the modal transitions were identified, the channel was then classified as being in the I mode if $t_g \le T_g$ and $t_b \le T_b$; in the H mode if $t_g \le T_g$ and $t_b > T_b$; and in the L mode if $t_g > T_g$ and $t_b \le T_b$ (Fig. 6). Cases in which a burst-terminating gap with $t_g > T_g$ occurred adjacent to a burst with $t_b > T_b$ were rare and considered to be modal transitions between L and H modes occurring between the burst and the gap (Fig. 6).

Channel mode assignments in this algorithm are based on the durations of two consecutive pairs of channel bursts and gaps rather than on the values of channel parameters (t_o, t_c, or P_o) averaged over some window
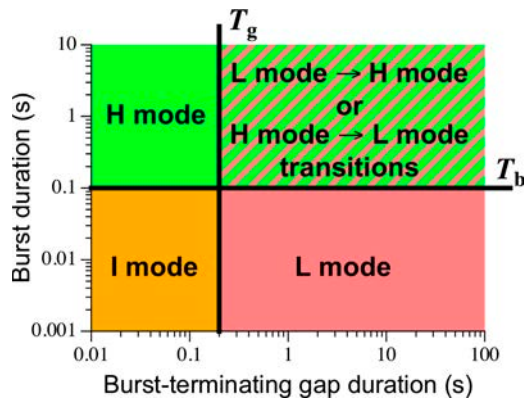
Figure 6. Scheme to determine channel gating mode based on the durations of adjacent channel bursts and burst-terminating gaps. The gating mode of the channel is assigned as indicated in a graph of channel burst duration t_b vs. duration of the adjacent burst-terminating gap t_g as shown. When a channel gap with $t_g > T_g$ occurred next to a channel burst with $t_b > T_b$ (area with yellow and green hatching), the channel is considered to undergo a modal transition from L to H mode (if the channel gap preceded the burst) or from H to L mode (if the burst preceded the gap).

(containing a constant number of openings and closings or lasting a constant time). Thus the assignment has high temporal resolution. Implementation of the hysteresis requirement improves the accuracy of the mode assignment by the algorithm.

Because mode assignment is based directly on only the durations of channel bursts (t_b) and burst-terminating gaps (t_g), there is no intrinsic restriction that the channel P_o within each gating mode should remain consistent among various ligand conditions. In fact, the values of the thresholds T_g and T_b used in the modal analysis only limit the value of channel P_o in the modes to: $0 \leq P_o^L \leq 0.33$; $0 \leq P_o^I \leq 1$; and $0.33 \leq P_o^H \leq 1$. Therefore, the consistency of the values of P_o^M for the three gating modes observed for various ligand conditions validates the identification of the three modes using the modal analysis algorithm.

Evaluation of InsP₃R Channel Gating Kinetic Parameters Overall and in Individual Gating Modes

Segment(s) of single-channel InsP₃R channel current records with stable baseline current levels were selected from each of the many experiments performed under various ligand concentration conditions (Table I). Segments shorter than 5 s were not used for modal analysis because their lengths are comparable to the mean modal dwell times $\langle \tau^M \rangle$, which causes an artifactual bias against long modal durations. Nevertheless, durations of selected segments from one experiment (showing the gating activity of one single InsP₃R channel) varied greatly, from 5 s to >750 s, depending on the stability of the giga-ohm seal between the patch-clamp micro-pipette and the isolated membrane patch, and the duration of

activity of the InsP₃R channel before inactivation or rundown. To provide proper weighing for experiments of different durations, the kinetic parameters for InsP₃R channel gating were evaluated using event-based statistics. This means that each opening (or closing) event from any experiment performed with the same set of ligand conditions was considered equivalent. Thus the mean open (or closed) duration $\langle t \rangle$ is given by

$$\langle t \rangle = \left\{ \sum_{j=1}^{M} \left(\sum_{i=1}^{N_j} t_{ij} \right) \right\} \left(\sum_{j=1}^{M} N_j \right)^{-1}, \qquad (A1)$$

where t_{ij} is the duration of the ith of N_j opening (or closing) events in the jth of M experiments performed in the set of ligand conditions in question (Fig. 3 E). Channel P_o (Fig. 3 A) is evaluated as the ratio of the sum of all open durations to the sum of all durations (open or closed). Similarly, the mean open (closed, burst, or gap) duration for each gating mode was evaluated by averaging with equal weight the durations of all the openings (closings, bursts, or gaps) in all the periods when the channel was determined to be in that mode by the modal analysis algorithm, regardless of which experiment the event was recorded in as long as the experiment was performed under the same set of ligand conditions (Fig. 3, F–I). Channel P_o^M was evaluated as the ratio of the sum of all open durations to the sum of all durations (open or closed) in a particular mode (Fig. 3 B). The mean modal dwell times $\langle \tau^M \rangle$ (Fig. 3 J) were evaluated using Eq. A1 with all dwell times of the mode from any experiment (using the same ligand conditions) weighted equally.

The duration distributions for channel openings and closings in general, and the distributions within each gating mode for channel openings, closings, bursts, and gaps, were all determined to be non-Gaussian by the Jarque-Bera (Jarque and Bera, 1987) and Kolmogorov-Smirnov (Khamis, 2000) tests. Thus, nonparametric statistical analyses were used to characterize and compare the distributions. The ranges of the distributions were described in terms of the standard deviations evaluated by the random bootstrap resampling method (Efron and Tibshirani, 1993; Mooney and Duval, 1993), and statistical significance of the differences between the durations was evaluated using the two-tailed nonparametric Wilcoxon-Mann-Whitney rank-sum test (Cheung and Klotz, 1997).

Because of the large numbers of events available from extensive experimental current records for each set of ligand conditions, the standard deviations of the durations t_c, t_o, t_o^M, t_c^M, t_b^M, and t_g^M are too small to be plotted in Fig. 3 (the error bars are all smaller than the symbols in the graphs). The errors in the values of channel P_o and P_o^M, derived from the durations, are also too small to be plotted. According to the nonparametric Wilcoxon-Mann-Whitney rank-sum test, most kinetic
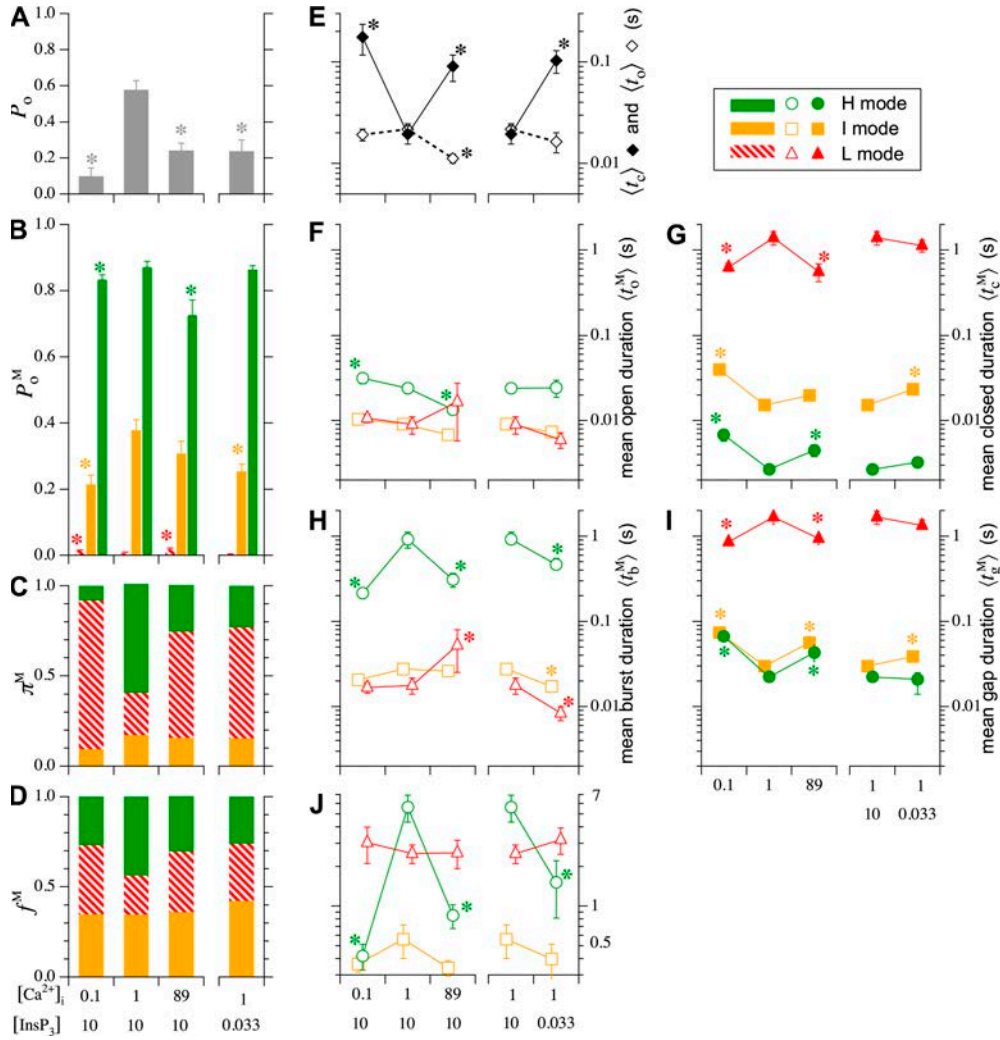
Figure 7. InsP₃R channel gating parameters in various [Ca²⁺]ᵢ and [InsP₃] evaluated using experiment-based statistics (see Appendix). The same channel gating parameters are plotted in the same panels with the same symbols and color code as in Fig. 3: (A) channel open probability P_o; (B) channel open probability in each of the three gating modes P_o^M; (C) relative prevalence π^M for the three gating modes; (D) relative frequency f^M of the gating modes; (E) mean overall channel opening $\langle t_o \rangle$ and closing $\langle t_c \rangle$ duration; (F–I) mean durations of channel opening $\langle t_o^M \rangle$, closing $\langle t_c^M \rangle$, bursts $\langle t_b^M \rangle$, and burst-terminating gaps $\langle t_g^M \rangle$, respectively, for the gating modes; (J) mean duration $\langle \tau^M \rangle$ of the gating modes. Error bars in (A, B, and E–J) indicate standard errors of the mean evaluated using experiment-based statistics (see Appendix). Parameters marked with asterisks are those observed in suboptimal ligand concentrations that are statistically significantly different from those observed in optimal [Ca²⁺]ᵢ (1 μM) and saturated [InsP₃] (10 μM).

quantities obtained under optimal (1 μM) Ca²⁺ᵢ and saturating (10 μM) InsP₃ were significantly different when compared with corresponding quantities obtained under other ligand conditions, low (100 nM) Ca²⁺ᵢ and saturating InsP₃, inhibitory (89 μM) Ca²⁺ᵢ and saturating InsP₃, optimal Ca²⁺ᵢ and subsaturating (33 nM) InsP₃.

Whereas event-based statistics may provide more accurate estimation of the channel gating parameters by taking into consideration the very different lengths of channel activity recorded in various experiments, the calculation gives no estimate of the experiment-to-experiment variability of the kinetic parameters. To gauge the reproducibility of the experiments, the kinetic parameters ($\langle t_c \rangle$, $\langle t_o \rangle$, $\langle t_o^M \rangle$, $\langle t_c^M \rangle$, $\langle t_b^M \rangle$, $\langle t_g^M \rangle$, or $\langle \tau^M \rangle$) were also evaluated by experiment-based statistics, so that

$$\langle t \rangle = \frac{1}{M}\left\{ \sum_{j=1}^{M}\left(\frac{1}{N_j}\sum_{i=1}^{N_j} t_{ij} \right) \right\} = \frac{1}{M}\left\{ \sum_{j=1}^{M}\langle t \rangle_j \right\}, \quad (A2)$$

where symbols are similar to those used in Eq. A1. As shown in the second half of Eq. A2, the average dura-

tions are evaluated as the mean of the mean durations from individual experiments. The channel open probabilities (P_o and P_o^M) derived by experiment-based statistics are similarly evaluated as the mean of channel open probabilities from individual experiments. More importantly, the standard deviations of these quantities derived by random bootstrap resampling provide some measure of the reproducibility of the experiments. The kinetic parameters and their standard deviations derived through experiment-based statistics are plotted in Fig. 7.

Despite the larger standard deviations of the kinetic quantities evaluated by experiment-based statistics, a comparison, using Wilcoxon-Mann-Whitney rank-sum test, of kinetic quantities obtained under optimal Ca²⁺ᵢ and saturating InsP₃ with those obtained in other ligand conditions revealed statistically significantly difference in a majority of the quantities.

Validation of Modal Gating Analysis Algorithm

The algorithm developed to analyze channel modal gating kinetics used three parameters: the minimum
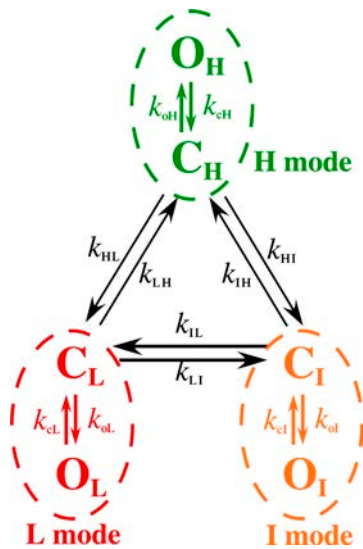
Figure 8. Schematic diagram showing the simplest completely-interconnected Markov kinetic model for three distinct gating modes. Each of the three modes (L, H, and I modes) consists of one closed (C_M) and one open (O_M) kinetic states, with state transition rates for channel opening (k_{oM}) and closing (k_{cM}) as tabulated. The three modes are completely interconnected through the closed kinetic states (C_H, C_I, and C_L) with six mode transition rates (k_{HL}, k_{HI}, k_{IL}, k_{IH}, k_{LI}, and k_{LH}). Through stochastic simulation, these kinetic rates were used to generate virtual channel current records, which in turn were used to check the accuracy of the modal analysis algorithm.

burst-terminating gap duration T_{gmin}, the limit of channel burst duration T_b, and the limit of gap duration T_g. The values of $T_{gmin} = 10$ ms, $T_b = 100$ ms, and $T_g = 200$ ms were selected by visual inspection of single InsP$_3$R channel current records and dwell time histograms. To check if the conclusions of the modal analysis are dependent on the choice of these parameters, we systematically examined the effects of using different sets of parameters on the results of our modal analysis. We found that for 7 ms $\leq T_{gmin} \leq 15$ ms, 50 ms $\leq T_b \leq 200$ ms, and 100 ms $\leq T_g \leq 300$ ms, the modal analysis algorithm still yielded three gating modes each with a distinct value of P_o (~0.8, 0.3, and 0.01 for H, I, and L modes, respectively) that were largely independent of ligand concentrations.

Because the gating activities and modal transitions of the channel are stochastic in nature, any modal analysis algorithm based on the kinetic properties of the channel (t_o and t_c) during a current record is inherently inaccurate to some extent. For example, although most channel closings are brief when the channel is in H mode, some long closings will inevitably occur even when the channel is in H mode, causing the mode analysis algorithm to misidentify the channel as being in the I or L mode. Moreover, even though the kinetics of modal transitions are significantly slower than that of channel gating: $\langle \tau^M \rangle >> \langle t_o \rangle, \langle t_c \rangle, \langle t_o^M \rangle$ or $\langle t_c^M \rangle$, our algorithm will not detect some brief residences of the

channel in a mode, particularly because of the hysteresis requirement used. The complexity of the modal analysis algorithm precludes an analytical approach to evaluate the error rate of the algorithm, i.e., the fraction of time when the algorithm misidentifies the mode of the channel. Furthermore, there is no detectable difference among the values of channel conductance for the InsP$_3$R channel in the three modes (Fig. 1) so that there is no assured means to derive the mode that a channel is in from the experimental patch-clamp current record. To estimate the error rate of the modal analysis algorithm, virtual channel current records were generated by stochastic simulation (Shuai et al., 2007) from the kinetic state of an InsP$_3$R channel in the simplest three-mode Markov model (Fig. 8). The simple model does not fully capture all the details of the observed InsP$_3$R channel modal behavior, but is simple enough that all the necessary state transition rates can be directly calculated from the experimentally observed modal properties of the channel ($\langle t_o^M \rangle, \langle t_c^M \rangle, \langle \tau^M \rangle, \pi^M$, and P_o^M). The virtual current records were analyzed using our modal analysis protocol. The error rate of our algorithm was estimated by comparing the results of the analysis with the known kinetic states of the channel from the simulation. The error rate of the algorithm was ~3.5% for all $[Ca^{2+}]_i$ examined (0.1, 1, and 89 μM). The error rate approximately doubled for every three-fold increase in the modal transition rates (I↔H, I↔L, and L↔H rates) used in the simulation. Thus, although there must be some inherent inaccuracies in modal transition rates used in the simulation because they were based on the modal properties derived by the modal analysis algorithm, the effects of such inaccuracies on the error rates are not significant. Finally, only 3% of a virtual current record generated for a channel in the H mode only (H→I and H→L rates = 0) and <1% of virtual current records generated for channels only in the I or L modes were misidentified. Thus, our modal analysis protocol identifies the kinetic modes of an InsP$_3$R channel from its current record with high accuracy and high temporal resolution.

REFERENCES

Adkins, C.E., and C.W. Taylor. 1999. Lateral inhibition of inositol 1,4,5-trisphosphate receptors by cytosolic Ca^{2+}. *Curr. Biol.* 9:1115–1118.

Atri, A., J. Amundson, D. Clapham, and J. Sneyd. 1993. A single-pool model for intracellular calcium oscillations and waves in the *Xenopus laevis* oocyte. *Biophys. J.* 65:1727–1739.

Auerbach, A., and C.J. Lingle. 1986. Heterogeneous kinetic properties of acetylcholine receptor channels in *Xenopus* myocytes. *J. Physiol.* 378:119–140.

Berridge, M.J. 1993. Inositol trisphosphate and calcium signalling. *Nature.* 361:315–325.

Berridge, M.J. 1997. Elementary and global aspects of calcium signalling. *J. Physiol.* 499:291–306.

Berridge, M.J., and R.F. Irvine. 1989. Inositol phosphates and cell signalling. *Nature.* 341:197–205.

Bezprozvanny, I. 1994. Theoretical analysis of calcium wave propagation based on inositol (1,4,5)-trisphosphate (InsP$_3$) receptor functional properties. *Cell Calcium.* 16:151–166.

Bezprozvanny, I., and B.E. Ehrlich. 1994. Inositol (1,4,5)-trisphosphate (InsP$_3$)-gated Ca channels from cerebellum: conduction properties for divalent cations and regulation by intraluminal calcium. *J. Gen. Physiol.* 104:821–856.

Blatz, A.L., and K.L. Magleby. 1986. Quantitative description of three modes of activity of fast chloride channels from rat skeletal muscle. *J. Physiol.* 378:141–174.

Boehning, D., S.K. Joseph, D.-O.D. Mak, and J.K. Foskett. 2001. Single-channel recordings of recombinant inositol trisphosphate receptors in mammalian nuclear envelope. *Biophys. J.* 81:117–124.

Bootman, M.D., M.J. Berridge, and H.L. Roderick. 2002. Activating calcium release through inositol 1,4,5-trisphosphate receptors without inositol 1,4,5-trisphosphate. *Proc. Natl. Acad. Sci. USA.* 99:7320–7322.

Bruno, W.J., J. Yang, and J.E. Pearson. 2005. Using independent open-to-closed transitions to simplify aggregated Markov models of ion channel gating kinetics. *Proc. Natl. Acad. Sci. USA.* 102:6326–6331.

Catacuzzeno, L., C. Trequattrini, A. Petris, and F. Franciolini. 1999. Bimodal kinetics of a chloride channel from human fibroblasts. *J. Membr. Biol.* 170:165–172.

Cheung, Y.K., and J.H. Klotz. 1997. The Mann Whitney Wilcoxon distribution using linked lists. *Statist. Sinica.* 7:805–813.

Dawson, A.P., E.J. Lea, and R.F. Irvine. 2003. Kinetic model of the inositol trisphosphate receptor that shows both steady-state and quantal patterns of Ca^{2+} release from intracellular stores. *Biochem. J.* 370:621–629.

De Young, G.W., and J. Keizer. 1992. A single-pool inositol 1,4,5-trisphosphate-receptor-based model for agonist-stimulated oscillations in Ca^{2+} concentration. *Proc. Natl. Acad. Sci. USA.* 89:9895–9899.

Delcour, A.H., D. Lipscombe, and R.W. Tsien. 1993. Multiple modes of N-type calcium channel activity distinguished by differences in gating kinetics. *J. Neurosci.* 13:181–194.

Delcour, A.H., and R.W. Tsien. 1993. Altered prevalence of gating modes in neurotransmitter inhibition of N-type calcium channels. *Science.* 259:980–984.

Dupont, G., and S. Swillens. 1996. Quantal release, incremental detection, and long-period Ca^{2+} oscillations in a model based on regulatory Ca^{2+}-binding sites along the permeation pathway. *Biophys. J.* 71:1714–1722.

Efron, E., and R. Tibshirani. 1993. An Introduction to the Bootstrap. Chapman & Hall, New York. 436 pp.

Fill, M., A. Zahradnikova, C.A. Villalba-Galea, I. Zahradnik, A.L. Escobar, and S. Gyorke. 2000. Ryanodine receptor adaptation. *J. Gen. Physiol.* 116:873–882.

Foskett, J.K., and D.-O.D. Mak. 2004. Novel model of calcium and inositol 1,4,5-trisphosphate regulation of InsP$_3$ receptor channel gating in native endoplasmic reticulum. *Biol. Res.* 37:513–519.

Foskett, J.K., C. White, K.H. Cheung, and D.-O.D. Mak. 2007. Inositol trisphosphate receptor Ca^{2+} release channels. *Physiol. Rev.* 87:593–658.

Fraiman, D., and S.P. Dawson. 2004. A model of IP$_3$ receptor with a luminal calcium binding site: stochastic simulations and analysis. *Cell Calcium.* 35:403–413.

Hirose, K., S. Kadowaki, and M. Iino. 1998. Allosteric regulation by cytoplasmic Ca^{2+} and IP$_3$ of the gating of IP$_3$ receptors in permeabilized guinea-pig vascular smooth muscle cells. *J. Physiol.* 506:407–414.

Imredy, J.P., and D.T. Yue. 1994. Mechanism of Ca^{2+}-sensitive inactivation of L-type Ca^{2+} channels. *Neuron.* 12:1301–1318.

Ionescu, L., K.H. Cheung, H. Vais, D.-O.D. Mak, C. White, and J.K. Foskett. 2006. Graded recruitment and inactivation of single InsP$_3$ receptor Ca^{2+}-release channels: implications for quantal Ca^{2+} release. *J. Physiol.* 573:645–662.

Jarque, C.M., and A.K. Bera. 1987. A test for normality of observations and regression residuals. *Int. Stat. Rev.* 55:163–172.

Kaftan, E.J., B.E. Ehrlich, and J. Watras. 1997. Inositol 1,4,5-trisphosphate (InsP$_3$) and calcium interact to increase the dynamic range of InsP$_3$ receptor-dependent calcium signaling. *J. Gen. Physiol.* 110:529–538.

Khamis, H.J. 2000. The two-stage delta-corrected Kolmogorov-Smirnov test. *J. Appl. Stat.* 27:439–450.

Luvisetto, S., T. Fellin, M. Spagnolo, B. Hivert, P.F. Brust, M.M. Harpold, K.A. Stauderman, M.E. Williams, and D. Pietrobon. 2004. Modal gating of human CaV2.1 (P/Q-type) calcium channels: I. The slow and the fast gating modes and their modulation by β subunits. *J. Gen. Physiol.* 124:445–461.

Magleby, K.L., and B.S. Pallotta. 1983a. Burst kinetics of single calcium-activated potassium channels in cultured rat muscle. *J. Physiol.* 344:605–623.

Magleby, K.L., and B.S. Pallotta. 1983b. Calcium dependence of open and shut interval distributions from calcium-activated potassium channels in cultured rat muscle. *J. Physiol.* 344:585–604.

Mak, D.-O.D., and J.K. Foskett. 1994. Single-channel inositol 1,4,5-trisphosphate receptor currents revealed by patch clamp of isolated *Xenopus* oocyte nuclei. *J. Biol. Chem.* 269:29375–29378.

Mak, D.-O.D., and J.K. Foskett. 1997. Single-channel kinetics, inactivation, and spatial distribution of inositol trisphosphate (IP$_3$) receptors in *Xenopus* oocyte nucleus. *J. Gen. Physiol.* 109:571–587.

Mak, D.-O.D., S. McBride, and J.K. Foskett. 1998. Inositol 1,4,5-trisphosphate activation of inositol trisphosphate receptor Ca^{2+} channel by ligand tuning of Ca^{2+} inhibition. *Proc. Natl. Acad. Sci. USA.* 95:15821–15825.

Mak, D.-O.D., S. McBride, and J.K. Foskett. 2001. Regulation by Ca^{2+} and inositol 1,4,5-trisphosphate (InsP$_3$) of single recombinant type 3 InsP$_3$ receptor channels. Ca^{2+} activation uniquely distinguishes types 1 and 3 InsP$_3$ receptors. *J. Gen. Physiol.* 117:435–446.

Mak, D.-O.D., S. McBride, V. Raghuram, Y. Yue, S.K. Joseph, and J.K. Foskett. 2000. Single-channel properties in endoplasmic reticulum membrane of recombinant type 3 inositol trisphosphate receptor. *J. Gen. Physiol.* 115:241–256.

Mak, D.-O.D., S.M. McBride, and J.K. Foskett. 2003. Spontaneous channel activity of the inositol 1,4,5-trisphosphate (InsP$_3$) receptor (InsP$_3$R). Application of allosteric modeling to calcium and InsP$_3$ regulation of InsP$_3$R single-channel gating. *J. Gen. Physiol.* 122:583–603.

Mak, D.-O.D., C. White, L. Ionescu, and J.K. Foskett. 2005. Nuclear patch clamp electrophysiology of inositol trisphosphate receptor Ca^{2+} release channels. *In* Methods in Calcium Signaling Research. J.W. Putney, Jr., editor. CRC Press, Boca Raton, FL. 203–229.

Mak, D.-O.D., J.E. Pearson, K.P.C. Loong, S. Datta, M. Fernández-Mongil, and J.K. Foskett. 2007. Rapid ligand-regulated gating kinetics of single 1,4,5-trisphosphate receptor Ca2+ release channels. *EMBO Rep.* 8:1044–1051.

Marchant, J.S., and C.W. Taylor. 1997. Cooperative activation of IP$_3$ receptors by sequential binding of IP$_3$ and Ca^{2+} safeguards against spontaneous activity. *Curr. Biol.* 7:510–518.

McManus, O.B., and K.L. Magleby. 1988. Kinetic states and modes of single large-conductance calcium-activated potassium channels in cultured rat skeletal muscle. *J. Physiol.* 402:79–120.

Mooney, C., and R. Duval. 1993. Bootstrapping: A Nonparametric Approach to Statistical Inference. Sage, Newbury Park, CA. 73 pp.

Moraru, I.I., E.J. Kaftan, B.E. Ehrlich, and J. Watras. 1999. Regulation of type 1 inositol 1,4,5-trisphosphate-gated calcium channels by InsP$_3$ and calcium: simulation of single channel kinetics based on ligand binding and electrophysiological analysis. *J. Gen. Physiol.* 113:837–849.

Naranjo, D., and P. Brehm. 1993. Modal shifts in acetylcholine receptor channel gating confer subunit-dependent desensitization. *Science.* 260:1811–1814.

Othmer, H.G., and Y. Tang. 1993. Oscillations and waves in a model of calcium dynamics. *In* Experimental and Theoretical Advances in Biological Pattern Formation. H.G. Othmer, J. Murray, and P. Maini, editors. Plenum Press, London. 295–319.

Petersen, C.C., E.C. Toescu, and O.H. Petersen. 1991. Different patterns of receptor-activated cytoplasmic Ca^{2+} oscillations in single pancreatic acinar cells: dependence on receptor type, agonist concentration and intracellular Ca^{2+} buffering. *EMBO J.* 10:527–533.

Popescu, G., and A. Auerbach. 2003. Modal gating of NMDA receptors and the shape of their synaptic response. *Nat. Neurosci.* 6:476–483.

Popescu, G., and A. Auerbach. 2004. The NMDA receptor gating machine: lessons from single channels. *Neuroscientist.* 10:192–198.

Popescu, G., A. Robert, J.R. Howe, and A. Auerbach. 2004. Reaction mechanism determines NMDA receptor response to repetitive stimulation. *Nature.* 430:790–793.

Qin, F., A. Auerbach, and F. Sachs. 2000a. A direct optimization approach to hidden Markov modeling for single channel kinetics. *Biophys. J.* 79:1915–1927.

Qin, F., A. Auerbach, and F. Sachs. 2000b. Hidden Markov modeling for single channel kinetics with filtering and correlated noise. *Biophys. J.* 79:1928–1944.

Rosales, R.A., M. Fill, and A.L. Escobar. 2004. Calcium regulation of single ryanodine receptor channel gating analyzed using HMM/ MCMC statistical methods. *J. Gen. Physiol.* 123:533–553.

Rothberg, B.S., R.A. Bello, L. Song, and K.L. Magleby. 1996. High Ca^{2+} concentrations induce a low activity mode and reveal Ca^{2+}-independent long shut intervals in BK channels from rat muscle. *J. Physiol.* 493:673–689.

Saftenku, E., A.J. Williams, and R. Sitsapesan. 2001. Markovian models of low and high activity levels of cardiac ryanodine receptors. *Biophys. J.* 80:2727–2741.

Shuai, J., J.E. Pearson, J.K. Foskett, D.-O.D. Mak, and I. Parker. 2007. A kinetic model of single and clustered IP$_3$ receptors in the absence of Ca^{2+} feedback. *Biophys. J.* 93:1151–1162.

Sneyd, J., and J.F. Dufour. 2002. A dynamic model of the type-2 inositol trisphosphate receptor. *Proc. Natl. Acad. Sci. USA.* 99:2398–2403.

Swatton, J.E., and C.W. Taylor. 2002. Fast biphasic regulation of type 3 inositol trisphosphate receptors by cytosolic calcium. *J. Biol. Chem.* 277:17571–17579.

Swillens, S., L. Combettes, and P. Champeil. 1994. Transient inositol 1,4,5-trisphosphate-induced Ca^{2+} release: a model based on regulatory Ca^{2+}-binding sites along the permeation pathway. *Proc. Natl. Acad. Sci. USA.* 91:10074–10078.

Swillens, S., P. Champeil, L. Combettes, and G. Dupont. 1998. Stochastic simulation of a single inositol 1,4,5-trisphosphate-sensitive Ca^{2+} channel reveals repetitive openings during 'blip-like' Ca^{2+} transients. *Cell Calcium.* 23:291–302.

Swillens, S., G. Dupont, L. Combettes, and P. Champeil. 1999. From calcium blips to calcium puffs: theoretical analysis of the requirements for interchannel communication. *Proc. Natl. Acad. Sci. USA.* 96:13750–13755.

Thorn, P., A.M. Lawrie, P.M. Smith, D.V. Gallacher, and O.H. Petersen. 1993. Local and global cytosolic Ca^{2+} oscillations in exocrine cells evoked by agonists and inositol trisphosphate. *Cell.* 74:661–668.

Tregear, R.T., A.P. Dawson, and R.F. Irvine. 1991. Quantal release of Ca^{2+} from intracellular stores by InsP$_3$: tests of the concept of control of Ca^{2+} release by intraluminal Ca^{2+}. *Proc. R. Soc. Lond. B. Biol. Sci.* 243:263–268.

Woods, N.M., K.S. Cuthbertson, and P.H. Cobbold. 1986. Repetitive transient rises in cytoplasmic free calcium in hormone-stimulated hepatocytes. *Nature.* 319:600–602.

Yakubovich, D., V. Pastushenko, A. Bitler, C.W. Dessauer, and N. Dascal. 2000. Slow modal gating of single G protein-activated K$^+$ channels expressed in *Xenopus* oocytes. *J. Physiol.* 524:737–755.

Yao, Y., J. Choi, and I. Parker. 1995. Quantal puffs of intracellular Ca^{2+} evoked by inositol trisphosphate in *Xenopus* oocytes. *J. Physiol.* 482:533–553.

Zahradnikova, A., and I. Zahradnik. 1996. A minimal gating model for the cardiac calcium release channel. *Biophys. J.* 71:2996–3012.

Zahradnikova, A., and I. Zahradnik. 1999. Analysis of calcium-induced calcium release in cardiac sarcoplasmic reticulum vesicles using models derived from single-channel data. *Biochim. Biophys. Acta.* 1418:268–284.

Zahradnikova, A., M. Dura, and S. Gyorke. 1999. Modal gating transitions in cardiac ryanodine receptors during increases of Ca^{2+} concentration produced by photolysis of caged Ca^{2+}. *Pflugers Arch.* 438:283–288.